The Astrophysical Journal Supplement Series, 141:13–21, 2002 July
© 2002. The American Astronomical Society. All rights reserved. Printed in U.S.A.

THE VLBA CALIBRATOR SURVEY—VCS1

A. J. Beasley[1]
Owens Valley Radio Observatory, California Institute of Technology, P.O. Box 968, Big Pine, CA 93513; tbeasley@ovro.caltech.edu

D. Gordon
Raytheon ITSS and NASA Goddard Space Flight Center, Code 926.9, Greenbelt, MD 20771; dgg@leo.gsfc.nasa.gov

A. B. Peck
Harvard-Smithsonian Center for Astrophysics, 60 Garden Street, Cambridge, MA 02138; apeck@cfa.harvard.edu

L. Petrov and D. S. MacMillan
NVI, Inc., and NASA Goddard Space Flight Center, Code 926, Greenbelt, MD 20771; pet@leo.gsfc.nasa.gov, dsm@leo.gsfc.nasa.gov

E. B. Fomalont
National Radio Astronomy Observatory, 520 Edgemont Road, Charlottesville, VA 22903; efomalon@nrao.edu

and

C. Ma
NASA Goddard Space Flight Center, Code 926, Greenbelt, MD 20771; cma@virgo.gsfc.nasa.gov
Received 2002 January 3; accepted 2002 January 22

ABSTRACT

A catalog containing milliarcsecond-accurate positions of 1332 extragalactic radio sources distributed over the northern sky is presented—the Very Long Baseline Array Calibrator Survey (VCS1). The positions have been derived from astrometric analysis of dual-frequency 2.3 and 8.4 GHz VLBA snapshot observations; in a majority of cases, images of the sources are also available. These radio sources are suitable for use in geodetic and astrometric experiments, and as phase-reference calibrators in high-sensitivity astronomical imaging. The VCS1 is the largest high-resolution radio survey ever undertaken and triples the number of sources available to the radio astronomy community for VLBI applications. In addition to the astrometric role, this survey can be used in active galactic nuclei, Galactic, gravitational lens, and cosmological studies.

Subject headings: astrometry — radio continuum: general — reference systems — surveys — techniques: interferometric

On-line material: machine-readable tables

1. INTRODUCTION

Accurate celestial and terrestrial reference frames play an important role in many areas of science. Celestial reference frames have been used historically for navigation (terrestrial and deep-space), time keeping and for studying the dynamics of solar system, Galactic and extragalactic objects. For over three decades, high-accuracy radio interferometry of extragalactic radio sources using the techniques of Very Long Baseline Interferometry (VLBI) has played a major role in defining these terrestrial and celestial frames (Sovers, Fanselow, & Jacobs 1998). Precise measurements of orientation, rotation and deformation of Earth's surface provides unique information concerning its internal structure, and allows detailed testing of geodynamic theories (e.g., plate tectonics) and studies of the major geophysical fluids (the atmosphere, oceans, and groundwater) (Eubanks 1993).

The International Earth Rotation Service (IERS[2]) was established in 1988 by the International Astronomical Union (IAU) and the International Union of Geodesy and Geophysics (IUGG) to serve the astronomical, geodetic, and geophysical communities by providing an International Celestial Reference System (ICRS) and an International Terrestrial Reference System (ITRS) to define fundamental inertial frames of reference for celestial and terrestrial positions. The current realizations of the ICRS and ITRS are the International Celestial Reference Frame (ICRF) (Ma et al. 1998) and the International Terrestrial Reference Frame (ITRF2000) (Altamimi, Sillard, & Boucher 2002). Physical connection of these two systems depends on accurate measurement of two celestial angles (the offset in longitude and obliquity of the celestial pole with respect to its position defined by the conventional IAU precession/nutation models—$\Delta\psi$ and $\Delta\epsilon$) and three Earth orientation parameters (EOPs): UT1 (changes in the length of day due to variations in the rotation of Earth), and the X and Y polar motion offsets.

The ICRF was adopted by the IAU as of 1998 January as the realization of the ICRS, replacing the FK5 (Fricke et al. 1988). It is a kinematic reference frame, based on the positions of distant quasars and active galactic nuclei, rather than a dynamical reference frame such as the FK5 frame (which incorporates Earth's motion, the mean equator and the dynamical equinox at some reference epoch). The origin of the ICRF is at the solar system barycenter, and its axes are defined by the directions to a set of extragalactic radio sources measured using VLBI. The ICRF axes are consistent with the J2000 alignment of the FK5 to within the accuracy of the FK5. The orientation of the ICRF is defined by the positions of the 212 defining sources included in the initial ICRF solution (Ma & Feissel 1997), with an estimated

[1] Combined Array for Research in Millimeter-wave Astronomy.
[2] See http://www.iers.org.

accuracy of 0.25 milliarcseconds (mas). A further 396 sources were included in Ma et al. (1998) as candidate ICRF sources to improve the catalog density, and subsequently 59 additional candidate sources were presented in ICRF-Extension 1 (ICRF-Ext.1) (IERS 1999). The data used to define the ICRF included over 2.2 million VLBI observations made between 1979 and 1995. Significant improvement of the ICRF will require VLBI monitoring of the mas structure of the current sources, and the addition of new sources to the frame solutions.

Astronomical imaging of weak radio sources using phase-referencing also relies on a dense and accurate grid of bright radio sources. Phase referencing (Beasley & Conway 1995) involves rapid (∼minutes) antenna position-switching between an astronomical target source and an adjacent (1°–5° separation) calibrator. By interpolating antenna-based phase, delay, and rate corrections derived from the calibrator observations to the weak target source, phase coherence can be extended indefinitely, allowing longer integration times and thermal-noise–limited imaging. To first order, unmodeled antenna-based geometric and electronic delays are removed. Second-order errors in this process increase with (*a*) switching time between observations of the calibrator, which depends on antenna slew rates, source brightness, and system sensitivity, and (*b*) the angular distance to the calibrator (i.e., a breakdown of isoplanicity). Dense calibrator grids are required to minimize these errors. Over the past 5 years, phase-referencing has allowed imaging of weak radio sources including GRBs (Taylor et al. 1999), radio stars (Beasley & Güdel 2000), and deep-field radio sources (Garrett et al. 2001). Another advantage of phase referencing is the astrometric registration of multiepoch observations, such as images of radio supernovae (Bartel et al. 2000), maser complexes (Herrnstein et al. 1999), and the Galactic center (Reid et al. 1999).

In this paper we present the results of a multiepoch dual-frequency Very Long Baseline Array (VLBA) survey—the VLBA Calibrator Survey (VCS1)—of 1811 VLBI sources identified on the basis of high-resolution Very Large Array observations. Some 1332 of these sources have not been previously measured in astrometric mode—their positions are presented here as the VCS1 catalog[3]). Future VLBA calibrator surveys (e.g., VCS2; E. B. Fomalont 2001, private communication) will build on this initial catalog. The goals of the survey were: (*a*) to increase the surface density of known geodetic-grade calibrators with mas-accurate positions in the northern sky, providing candidate sources for future extensions of the ICRF; (*b*) to facilitate routine phase-referencing to most regions of the northern and equatorial sky, allowing high-resolution radio imaging of weak scientific targets; and (*c*) to provide a uniform image database at 2.3 and 8.4 GHz for use in scientific applications, including AGN and gravitational lensing studies, and cosmology. Milliarcsecond-accurate positions in the reference frame of the ICRF and a selection of dual-frequency images of VCS1 sources are presented. In § 2 we describe the VCS1 sample and the survey observations and present a selection of survey images. In §§ 3 and 4 we discuss the astrometric analysis of the VCS1 sample and examine ongoing efforts to use VCS1 for scientific research and to expand it through the Galactic plane and to higher frequencies.

[3] See http://www.nrao.edu/vlba/VCS1.

2. DATA AND REDUCTION

2.1. *Observations*

The VCS1 observations were carried out in 10 24 hr sessions (epochs) spanning the period 1994 August to 1997 August. A description of the VLBA can be found in Napier (1994). VCS1 observations used the VLBA dual-frequency geodetic mode, observing simultaneously at 2.3 and 8.4 GHz. This is enabled by a dichroic mirror permanently positioned over the 2.3 GHz receiver, reflecting the higher frequency radiation toward a deployable reflector leading to the 8.4 GHz receiver. From each receiver four baseband frequency channels (BBCs) were recorded over a large spanned bandwidth (100 MHz at 2.3 GHz, 400 MHz at 8.4 GHz), to provide precise measurements of group delays for astrometric processing. Relevant parameters for the VCS1 epochs are indicated in Table 1. For epochs 1–4 the data recording rate was 64 Mb s^{-1}; growth of the VLBA operational capabilities during 1996 allowed 128 Mb s^{-1} recording for epochs 6–10. Typical VLBA antenna system temperatures and efficiencies at 2.3 and 8.4 GHz are ∼30–40 K and 50%. During each epoch, typically one or two antennas exhibited poor performance due to local weather conditions.

To allow accurate imaging and position estimation, two or three 60–90 s snapshot observations of each calibrator candidate were made. The VCS1 sample was observed in declination strips, as indicated in Table 1. In each declination strip the observations were sequenced to maximize the number of VLBA antennas on source using customized scheduling software. During each epoch, six or seven periods of 30 minutes were used to observe ∼10 geodetic-grade reference sources spanning a wide range of elevations and azimuths to assist in the astrometric processing of the survey. To schedule these reference sources, an elevation-weighted simulated annealing algorithm was developed. For a given date and time, this algorithm identifies sources visible to all VLBA antennas and generates a preferred sample spanning a wide range of antenna elevations and azimuths, giving higher weight to the outlying VLBA stations, i.e., those involving longer baselines which provide the high-

TABLE 1
VCS1 Observations

Epoch	Date	δ[a] (deg)	N_{srcs}[b]	Mb s^{-1}	Notes
1.....	1994 Aug 12	50–61	216	64	
2.....	1995 May 19	61–79	215	64	
3.....	1995 Jul 15	00–12	216	64	
4.....	1996 Mar 13	12–24	216	64	[c]
5.....	1996 May 15	24–34	192	128	
6.....	1996 June 07	34–44	192	128	
7.....	1996 Aug 10	44–51	192	128	[c]
8.....	1997 May 07	00– −14	192	128	
9.....	1997 Jul 02	−14– −28	191	128	
10.....	1997 Aug 27[d]	−18– −30	160	128	
	1997 Aug 27	78–90	32	128	

[a] Declination range observed during each epoch.
[b] Number of VCS1 candidates sources observed per epoch. Approximately 10% of the sample was observed in multiple epochs to assess astrometric accuracy.
[c] Three epochs (1996 January 2, 1997 March 21, and 1997 April 4) were abandoned due to poor weather at a majority of the VLBA sites.
[d] Two declination ranges were observed during this epoch.

est astrometric accuracy. After selection, the list of reference sources is ordered in time using a simulated annealing algorithm (Press et al. 1992) to give the minimum antenna slew path through the sources, ignoring azimuth cable unwrapping.

2.2. *VCS1 Sample Selection*

A sample of candidate calibrators was selected from the Jodrell Bank—VLA Astrometric Survey (JVAS) (Patnaik et al. 1992b; Browne et al. 1998; Wilkinson et al. 1998; J. Winn et al. 2002, in preparation), an astrometric snapshot survey of compact radio sources performed with the NRAO Very Large Array during the period 1990–1993. The primary goal of JVAS was to provide phase calibrators with accurate positions for use in radio astronomy, in particular for the MERLIN array, although the survey has also been used to identify gravitationally lensed systems, e.g., King et al. (1999). The JVAS sample was originally derived from the NRAO Green Bank 1.4 and 5 GHz surveys (Condon & Broderick 1985, 1986; Condon, Broderick, & Seielstad 1989), selecting sources with 5 GHz flux densities greater than 200 milliJansky (mJy), spectral indices α greater than -0.5 ($S \propto \nu^{\alpha}$), and Galactic latitude $|b|$ greater than $2^{\circ}.5$. These criteria were adopted to select bright, compact extragalactic radio sources with mas-scale core emission. The JVAS catalog contains 2118 sources in the northern hemisphere; a southern hemisphere extension of $\sim$1000 sources (0° to -30°) is in preparation (J. Winn et al. 2002, in preparation). The positional accuracy of JVAS sources varies from 12 to 55 mas (1 σ errors), depending on declination and observing conditions. The celestial frame in which the JVAS positions have been specified is not formally defined, but it appears consistent with the ICRF at the mas level. Systematic offsets due to frame alignment and/or definition are considerably smaller than the observational errors in the individual JVAS positions.

To identify a sample of calibrator candidates suitable for high-resolution applications, we selected sources from the JVAS satisfying two criteria: (*a*) JVAS structure estimates indicating pointlike emission, suggesting compact emission on scales of 10–30 mas; and (*b*) 8.4 flux density $\geq$200 mJy (150 mJy in epochs 1 and 2), i.e., suitably bright for phase-referencing. An input sample of 1811 JVAS sources was selected and observed during the VCS1 epochs. The positional accuracy of the JVAS catalog is sufficient to provide initial correlation positions for VLBI purposes. We note that the VCS1 sample is a representative but not statistically complete sample of compact flat-spectrum sources, due to incompleteness in the original JVAS survey (Patnaik et al. 1992b) and possible source variability since the Green Bank and JVAS surveys.

Throughout the survey, a sample of 57 bright geodetic-grade reference sources were observed to provide estimates of epoch-to-epoch and absolute positional accuracy and to bootstrap atmospheric and instrumental error estimates for the individual epochs. All of these sources are included in the ICRF and ICRF-Ext. 1 catalogs (Ma & Feissel 1997). A total of 387 (out of 667 cataloged) ICRF-Ext. 1 sources were observed during this survey, and new position estimates were made using dual-frequency VCS1 observations for 72 ICRF-Ext. 1 sources with cataloged position errors greater than 0.5 mas rms. Figure 1 shows the celestial distribution of the 667 ICRF-Ext. 1 sources (*top*) and the 1332 VCS1 calibrators (*bottom*).

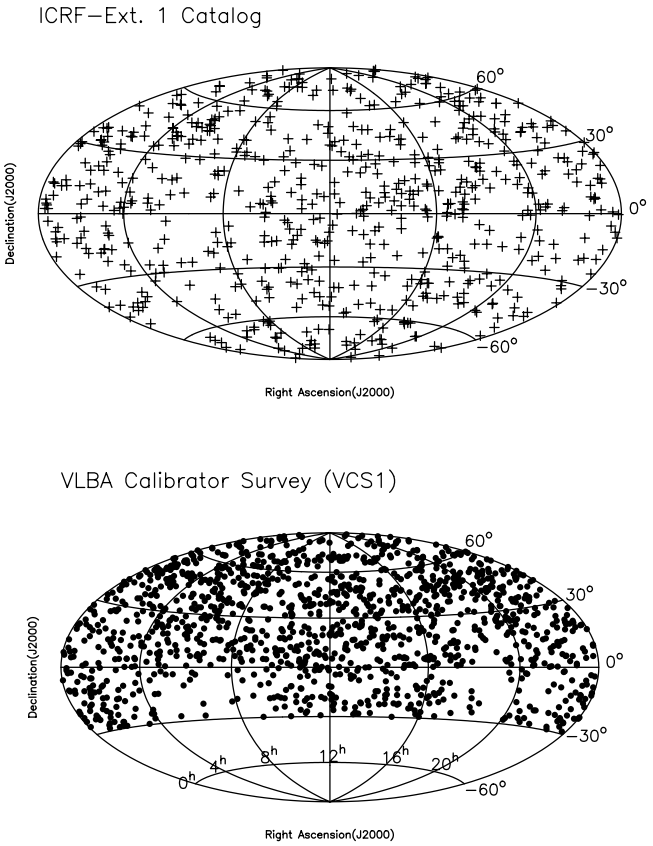

FIG. 1.—Equal-area projection of celestial distribution of ICRF-Ext. 1 (667 sources, *top*) and VCS1 catalogs (1332 sources, *bottom*).

2.3. *Calibration and Imaging*

Amplitude and initial phase calibration of the survey was done using the National Radio Astronomy Observatory Astronomical Imaging Processing System (AIPS) software. Absolute amplitude calibration is achieved using internal noise calibration sources at the VLBA antennas. After fringe fitting, the amplitude and phase-calibrated data were exported to FITS format for imaging purposes. Automated imaging of the VCS1 sources to enable on-line access was carried out using the Caltech DIFMAP package. Starting with a point source model, iterations of CLEAN and self-calibration procedures were carried out until noiselike residuals were encountered, at which point a final naturally weighted image was produced. A selection of the VCS1 candidate images is shown in Figure 2. The typical image rms is 2–3 mJy, with a dynamic range of $\sim$30:1 or better. Of the total 1811 sources observed, approximately 1300 sources (70%) imaged automatically at 8.4 GHz. Additional sources were manually imaged. Calibrator candidates which failed to image generally had too little data, or were strongly resolved on a majority of VLBA baselines, indicating source sizes of greater than 10–20 mas. The images and *u-v* radius plots for the VCS1 can be accessed on-line via a graphical search engine[4]).

[4] See http://magnolia.nrao.edu/vlba_calib/index.html.

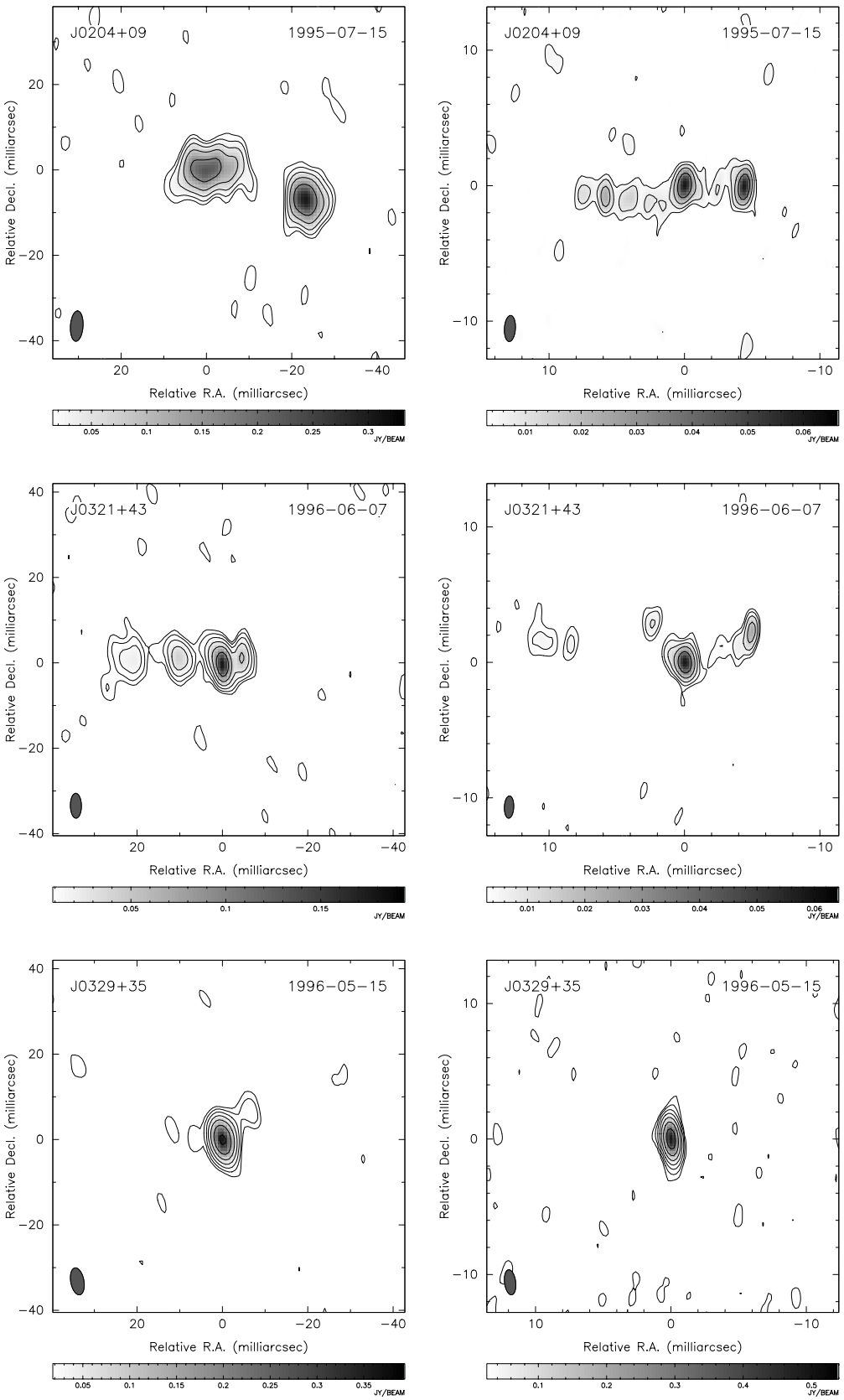

FIG. 2.—VCS1 image selection, 2.3 GHz (*left*), 8.4 GHz (*right*). Contour levels at −1, 1, 2, 4, 8, 16, 32, 64, 128 (and subsequent powers of 2) times the lowest contour level indicated. *First row*, J0204+0903 peak/integrated/lowest contour flux densities (P/I/L) 303/1480/10 mJy (2.3 GHz), 61/341/4 mJy (8.4 GHz); *second row*, J0321+4359: P/I/L 177/430/3 mJy (2.3 GHz), 58/169/2 mJy (8.4 GHz); *third row*, J0329+3510: P/I/L 358/465/5 mJy (2.3 GHz), 490/537/5 mJy (8.4 GHz); *fourth row*, J1310+3220: P/I/L 3340/3700/20 mJy (2.3 GHz), 2610/3250/20 mJy (8.4 GHz); *fifth row*, J1415+1334: P/I/L 220/867/5 mJy (2.3 GHz), 1210/1360/7 mJy (8.4 GHz); *sixth row*, J2029+4636: P/I/L 60/241/3 mJy (2.3 GHz), 55/100/3 mJy (8.4 GHz).

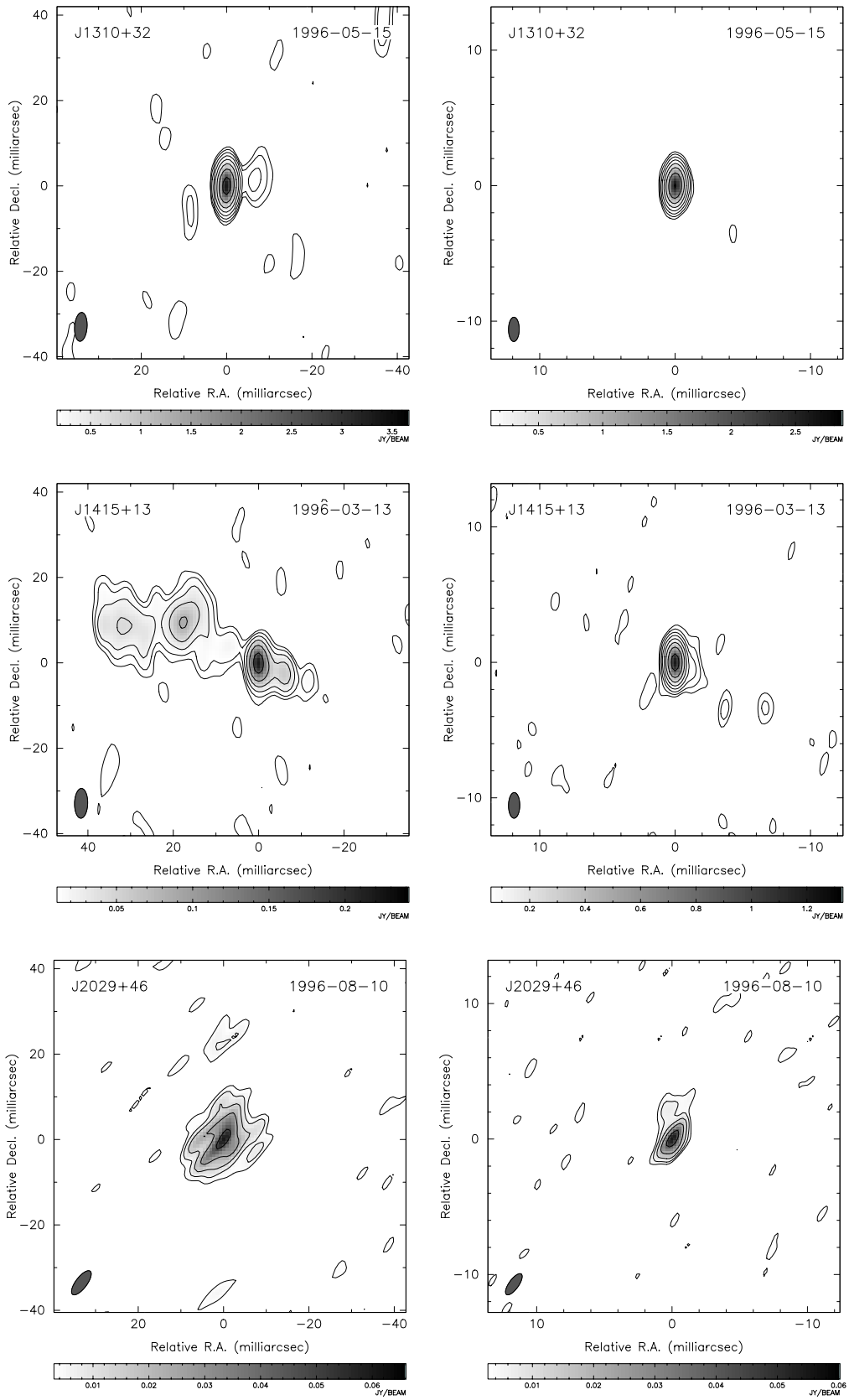

FIG. 2.—*Continued*

3. ASTROMETRY

Astrometric processing of the VCS1 was performed at the NASA Goddard Space Flight Center using AIPS and the CALC/SOLVE software packages. Each epoch and each frequency band (2.3 and 8.4 GHz) was processed independently in AIPS. Electronic phase offsets were applied to the amplitude calibrated visibilities using either measured phase tone phases (epochs 4–10) or using phase offsets determined by fringe fitting a reference scan on a bright source (epochs 1–3). Phase and amplitude variations across the individual BBCs were estimated and corrected using a reference scan on a bright source. Individual baselines were then fringe fitted in AIPS to obtain residual single-band delays, multiband (bandwidth synthesis) delays, phase delay rates, and fringe phases. These quantities were then combined with the correlator model to obtain total group delays, delay rates, and phases. Finally, the totals were shifted from geocentric quantities to the standard geodetic/astrometric reference-station baseline observables, and were written out in a form suitable for import into the CALC/SOLVE analysis package. CALC/SOLVE is a geodetic/astrometric VLBI analysis package, developed and maintained by the GSFC VLBI group and other partners for the international geodetic/astrometric community.

CALC computes theoretical delays and delay rates using astronomical and geophysical models following the IERS 1996 Conventions (McCarthy 1996), and is used by numerous correlators around the world, including the VLBA, Mark III, Mark IV, JIVE, DRAO, and ATNF correlators. SOLVE performs a least squares fit between the observed and theoretical delays and delay rates, allowing numerous parameters to be adjusted. Ionosphere-corrected linear combinations of the observed 2.3 and 8.4 GHz band group delays were used in the analysis. Initially, SOLVE analyses were made of each epoch to resolve group delay ambiguities, to eliminate outliers (2%–4% of observations), and to estimate preliminary VCS1 source positions. When all epochs were ready, a final SOLVE analysis was made of all VCS1 epochs simultaneously to estimate (*a*) final source positions; (*b*) positions of all stations except one assumed as a reference; (*c*) rate of change of UT1; (*d*) nutation offsets; (*e*) troposphere path delays and station clock behavior; and (*f*) east-west and north-south troposphere gradients and their derivatives. Clocks and tropospheres were modeled by linear splines with 60 minute intervals, with constraints on their rate of change imposed with reciprocal weights of 50 ps hr^{-1} and 5×10^{-14} s s^{-1}, respectively.

In total, 1811 radio sources were observed in the VCS1 campaign. Two known gravitational lenses, 0218+357 and 1830−211, as well as the radio source 0001−121 were excluded from the astrometric solution since the fringing process for different observations apparently chose peaks which corresponded to different source components. To align the VCS1 positions with the reference frame defined by ICRF-Ext. 1, the positions of 315 ICRF-Ext. 1 reference sources observed were fixed at their catalog values during the astrometric processing. These fixed sources have position error ellipses with semimajor axes of 1.0 mas or less (IERS 1999).

The positions of 1370 sources with three or more group delays at both 2.3 and 8.4 GHz were estimated from the VCS1 data. An additional 34 sources had fewer than two successful observations at 2.3 GHz but more than two good observations at 8.4 GHz. A supplementary solution using only 8.4 GHz group delays was made including these 34 sources. For nine sources with fewer than 10 dual-frequency delays but considerably more 8.4 GHz delays, the positions from the 8.4 GHz only solution were also taken as being more reliable. Since VCS1 observations were made during the years of solar minimum, errors due to uncorrected ionospheric delays in the 8.4 GHz data were relatively small. The final VCS1 catalog contains positions of 1289 sources from the dual-frequency solutions, and 43 source positions derived from the 8.4 GHz only solution.

In Table 2 the survey information for the first 10 sources in the VCS1 catalog is shown, including J2000 and IVS B1950 source names, J2000 positions and position errors, the correlation r between the position error estimates in right ascension and declination, the number of observations included (N_{obs}) and the solution origin (X/S, solution incorporates both 2.3 and 8.4 GHz group delays; X-only, solution incorporates only 8.4 GHz group delays; X+, solution incorporates only 8.4 GHz group delays: 2.3 GHz group delays were available, but the number of 2.3 GHz group delays was significantly less than the number of 8.4 GHz group delays). The parameter r is a measure of the covariances of the right ascension and declination position estimates, with high values of $|r|$ (≥ 0.5) generally indicating that the array geometry was not optimal during the observations of

TABLE 2
VCS1 Catalog Sample

J2000 Name	IVS B1950 Name	Right Ascension (J2000)	Declination (J2000)	σ_{ra} (mas)	σ_{decl} (mas)	r	N_{obs}	Code
J0000+4054	2358+406	00 00 53.081551	+40 54 01.79335	2.38	2.11	−0.16	22	X/S
J0001−1551	2358−161	00 01 05.328752	−15 51 07.07583	0.62	0.95	−0.75	58	X/S
J0001+1914	2358+189	00 01 08.621564	+19 14 33.80177	0.44	0.48	0.00	101	X/S
J0003−1927	0000−197	00 03 18.675008	−19 27 22.35478	0.65	1.00	−0.22	76	X/S
J0003+2129	0000+212	00 03 19.350020	+21 29 44.50760	0.74	1.21	−0.26	35	X/S
J0004−1148	0001−120	00 04 04.914996	−11 48 58.38567	0.42	0.51	0.05	81	X/S
J0004+4615	0001+459	00 04 16.127657	+46 15 17.96994	0.71	0.72	0.10	75	X/S
J0005+5428	0002+541	00 05 04.363490	+54 28 24.92651	1.43	1.17	0.46	60	X/S
J0005−1648	0002−170	00 05 17.933794	−16 48 04.67886	0.57	0.94	−0.55	64	X/S
J0005+0524	0002+051	00 05 20.215569	+05 24 10.80084	2.10	2.22	−0.10	26	X/S

Notes.—Units of right ascension are hours, minutes, and seconds, and units of declination are degrees, arcminutes, and arcseconds. Table 2 is available in its entirety in the electronic edition of the *Astrophysical Journal Supplement*. A portion is shown here for guidance regarding its form and content.

TABLE 3
VCS1 OBSERVATIONSVCS1 WEAK OR NONDETECTIONS

JVAS J2000 Source Names					
J0003+4807	J0003−1149	J0030+5904	J0032+1953	J0045+4555	J0121+1127
J0127+7323	J0145+5810	J0151+5454	J0214+5144	J0221+3556	J0308+6955
J0332+6753	J0344+6518	J0354+6621	J0401+0413	J0418+5457	J0426+6825
J0429+6710	J0448+5921	J0505+6406	J0524+7034	J0544+5258	J0610+7801
J0612+6225	J0642+5247	J0647+5446	J0657+5741	J0714+7408	J0718+6651
J0733+5605	J0749+5750	J0752+5808	J0754+7140	J0754+5324	J0757+6110
J0809+5341	J0814+6431	J0836+0052	J0853+6828	J0853+6722	J0855+5751
J0856+7146	J0907+6644	J0917+6530	J0921+1350	J0929+7304	J0943+6150
J0948+0022	J1011+6529	J1027+7428	J1032+5610	J1034+6832	J1124+6555
J1132+0034	J1148+5254	J1154+5934	J1156+7306	J1200+5300	J1203+6031
J1204+5228	J1210+6422	J1219+6344	J1233+5026	J1241+5458	J1247+7124
J1256+5652	J1258+5421	J1316+6726	J1330+5202	J1340+6923	J1350+6132
J1353+6324	J1401+5835	J1407+7628	J1411+5917	J1410+6216	J1420+1703
J1429+6316	J1448+5326	J1451+6357	J1507+5857	J1520+5635	J1524+7336
J1542−0927	J1541+5348	J1548+7845	J1557+4522	J1556+7420	J1558+5625
J1603+6945	J1610+7809	J1629+6757	J1628+7706	J1651+5805	J1656+5321
J1705+7756	J1746+6421	J1745+6703	J1757+7539	J1803+0934	J1825+5753
J1833−2103	J1850+4959	J1928+6814	J1926+7706	J1930+5948	J1938+6307
J1952+4958	J2007+7452	J2015+4628	J2014+6553	J2052+6858	J2100+5612
J2106+6004	J2129+6819	J2203+7151	J2209−2331	J2223+6249	J2232+6249
J2307+1450	J2322+6911	J2331+4522	J2343+7003	J2347+5142	J2349+7517

this source, leading to poor position estimation. There were 126 sources not detected at either band, or yielding only one measurement of group delay, and were therefore not used in the astrometric solution (these sources are listed in Table 3).

The VCS1 catalog, and a catalog containing improved positions for the 72 ICRF-Ext. 1 sources solved for in the VCS1 dual-frequency astrometric analysis (Table 4), are available on-line.[5] Complete versions of Table 2 and Table 4 are also available in the on-line edition of the Journal.

3.1. *Error Analysis*

The observing methodology of the VCS1 was significantly different from that used by traditional geodetic/astrometric VLBI experiments. The major source of errors in geodetic/astrometric experiments is from fluctuations in the troposphere path delays, which are estimated from the observations themselves. In order to separate the troposphere from other parameters in the least-squares solution, the VCS1 observing schedules included observations of sources at both low and high elevation for each station every hour, and to cover the sky as uniformly as possible. Figure 3 presents the sky coverage for a VLBI antenna (the North Liberty VLBA station) during a typical geodetic/astrometric experiment and during a VCS1 epoch. The VCS1 was observed in declinations strips, leading to significantly less uniform sky coverage. Therefore, one could expect that the VCS1 catalog positions may have some systematic errors due to poorer estimates of troposphere zenith path delay and horizontal troposphere gradients.

[5] See http://www.nrao.edu/vlba/VCS1.

TABLE 4
VCS1 ICRF-EXT. 1 SOURCE CATALOG

This table is available only on-line as a machine-readable table

In order to investigate the presence of systematic errors of the VCS1 catalog a trial solution was made. The positions of all sources except the 57 reference sources were estimated, including 296 sources that were in both the VCS1 and ICRF-Ext. 1 source lists. Vectors of the differences in positions between the trial solution and ICRF-Ext. 1 for 272 sources with semimajor error axes less than 2 mas are shown in Figure 4. No pattern is apparent, suggesting that systematic effects in the VCS1 astrometric analysis are small.

It has been found from analysis of different geodetic results (Ryan et al. 1993), such as baseline lengths, Earth orientation parameters, source positions, etc., that the formal errors of these estimated parameters should be scaled up by the factor of 1.5. Analysis of source positions have indicated that the actual errors generally have a noise floor (Ma et al. 1998). Therefore, source positions errors in the ICRF catalog were inflated:

$$\sigma_r = \sqrt{(1.5\sigma_f)^2 + a^2}\,, \tag{1}$$

where σ_r stands for the reported uncertainties, σ_f stands for the formal errors, and a stands for the additive noise term.

For the VCS1 we have adopted a similar error model. We used the differences between the trial solution and the ICRF-Ext. 1 catalog and obtained an additive noise term of 0.4 mas for VCS1 source positions derived using ionosphere-free joint dual-frequency group delays, and a noise term of 1.0 mas when 8.4 GHz only delays were used. This additive term makes χ^2 per degree of freedom of the differences in source positions between the trial solution and ICRF-Ext. 1 approximately unity. Reported uncertainties of source positions in the VCS1 catalog were inflated using equation (1) and these values of the additive noise terms.

A histogram of the distribution of the semimajor axes of the inflated error ellipses is presented in Figure 5. In the VCS1 catalog 53% of sources catalog have errors less than 1 mas and only 8% of sources have errors greater than 10 mas. The median value of the VCS1 position error distribution is

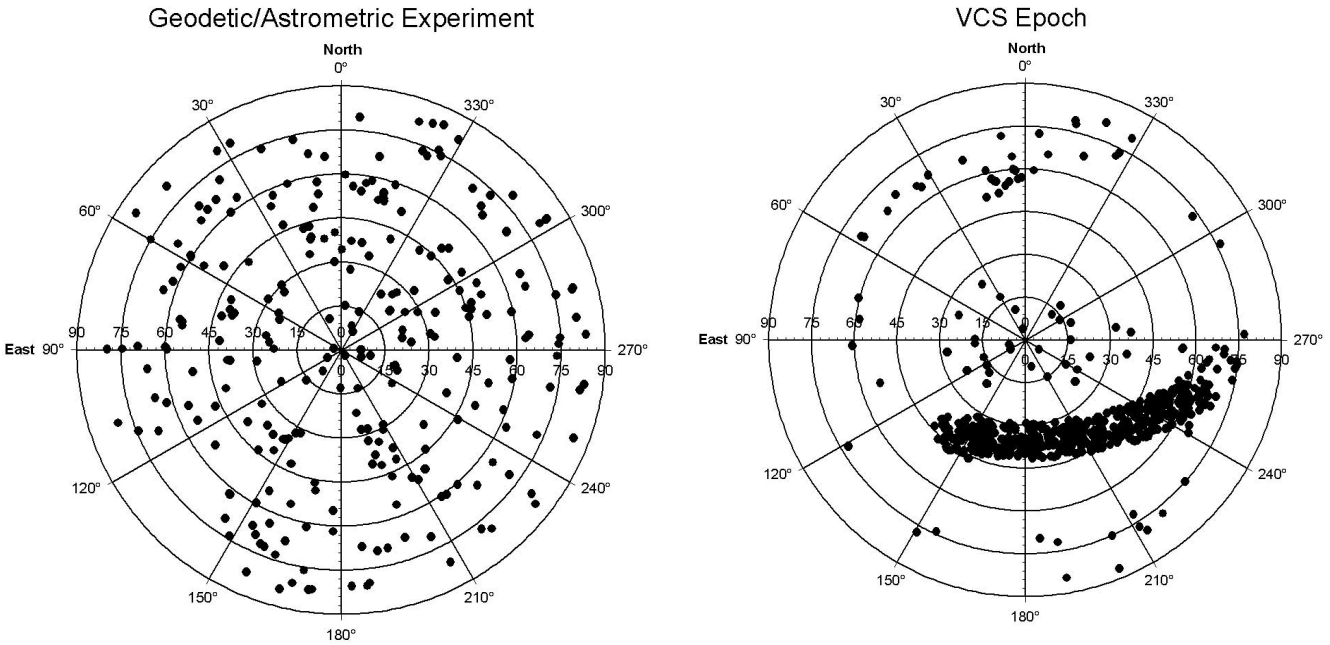

FIG. 3.—Azimuth/elevation distribution of observed sources for a central VLBA antenna during a typical geoodetic/astrometric experiment (*left*) and VCS1 epoch (*right*).

~0.9 mas, while the median error of the ICRF-Ext. 1 catalog is 0.5 mas. Typical geodetic/astrometric experiments focus on source samples with simple or known brightness distribution, and have much better sky coverage. The complex effects of undetermined and variable source structure on astrometric positions have been studied recently (Charlot 1990; Fey & Charlot 2000) and may be assessed for the VCS1 in the future using the results of automated imaging and follow–up observations. Multiyear phase-referencing observations using compact extragalactic reference sources taken from VCS1, ICRF-Ext. 11, or other catalogs may be affected by source evolution and variability at the sub-mas level, and therefore careful monitoring of reference source structure or the use of multiple reference sources is required in high-precision astrometric applications.

4. DISCUSSION

The mas–accurate positions for compact bright extragalactic radio sources presented in this survey will enable phase–referencing VLBI imaging of weak astronomical targets over large areas of the northern sky. The combined ICRF-Ext. 1 and VCS1 sky density is sufficient to provide a calibrator within 3° of a random location north of −30°

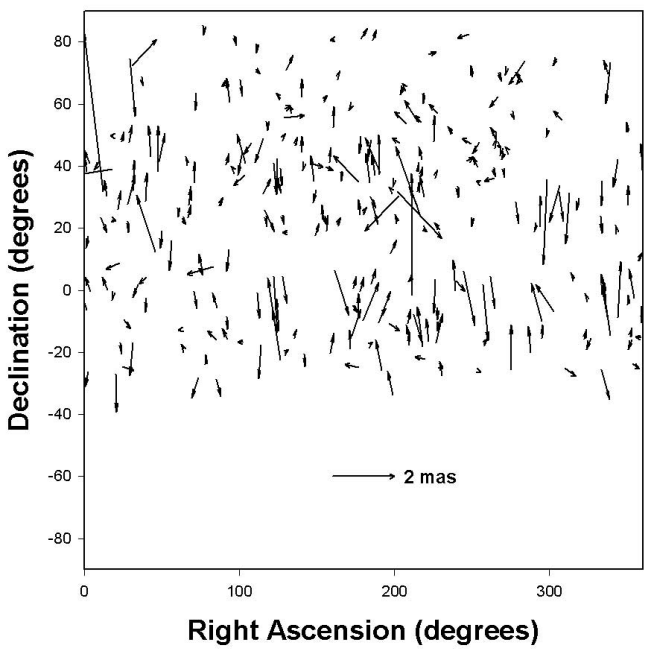

FIG. 4.—Position-difference vectors for VCS1 trial-reduction survey positions vs. ICRF-Ext. 1 catalog positions. A 2 mas arc length is indicated. No systematic effect is apparent, suggesting that the observing technique used has not systematically biased the VCS1 positions.

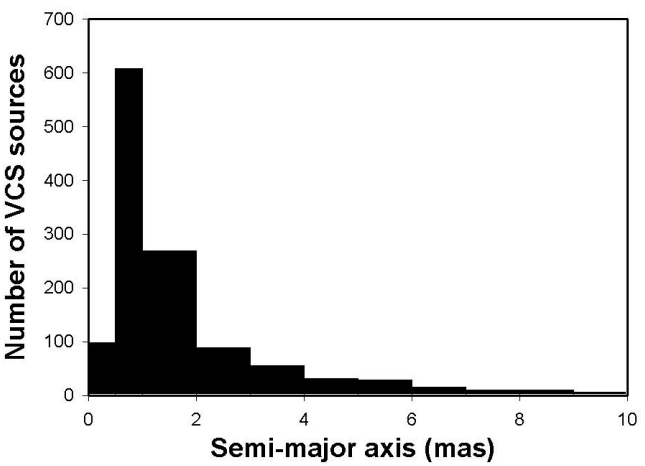

FIG. 5.—Histogram of the distribution of the semimajor axes of the inflated error ellipses for the 1332 VCS1 calibrators. 53% of survey sources have errors less than 1 mas, 8% greater than 10 mas.

declination approximately 75% of the time, and within 5° in 96% of cases. Experiments requiring high astrometric accuracy, or in cases where no suitable cataloged VLBI calibrator can be found within a few degrees, may use weaker continuum sources close to the astronomical target if sufficient data recording bandwidth is available. These weaker continuum sources may be identified from lower resolution surveys such as the NRAO VLA Sky Survey (Condon et al. 1998). Short- and long-term source variability may vary the flux densities of the VCS1 sources by tens of percent in extreme cases, so weaker calibrators should be examined before use in critical applications.

Use of the VCS1 in scientific studies has already commenced. The parent survey to VCS1—JVAS—has been extensively used to search for gravitationally lensed systems (Patnaik et al. 1992a; King et al. 1999). The existence or absence of gravitational-lens pairs on mas scales can be used to place limits on the cosmological abundance of supermassive compact objects in the mass range $\sim 10^6$ to $10^8\ M_\odot$ (Wilkinson et al. 2001). Current studies based on samples of $\sim$300 sources indicate that such objects cannot make up more than 1% of the closure density of the universe. This suggests that a population of supermassive black holes forming soon after the Big Bang does not contribute significantly to the dark matter content of the universe.

Examination of the VCS1 images to identify compact-symmetric objects (CSOs) has been carried out (Peck & Taylor 2000), doubling the number of these objects available for follow-up observations, including the detection of neutral hydrogen absorption toward the radio components of some CSOs (Peck et al. 2000), which may indicate the presence of an obscuring atomic torus in the nucleus of these objects. CSOs have also been found to be remarkably stable flux calibrators (Fassnacht & Taylor 2001), so larger samples will prove valuable for VLA and VLBA flux monitoring experiments, such as measuring time delays in gravitationally lensed sources.

Additional surveys based on the VCS1 to identify sources suitable as geodetic and phase-referencing calibrators at high frequencies (22–90 GHz), and throughout the Galactic plane, have recently commenced (E. B. Fomalont 2001, private communication). Proper-motion studies of Galactic objects such as pulsars (Brisken et al. 2000) depend on dense grids of suitable low-frequency calibrators at low Galactic declinations, which VCS1 does not cover. The results of these efforts should further benefit the geodetic and astrometric communities.

At the present time, radio observations are the most accurate way to define the ICRS; however, in the future optical observations will likely play an important role. The *Hipparcos* stellar reference frame (Perryman et al. 1997) has been aligned with the ICRF to within 0.6 mas offset and 0.25 mas in rotation at epoch 1991.25 (Kovalevsky et al. 1997) and represents the optical realization of the ICRS. Over the next two decades, new optical interferometers and astrometry missions such as the NASA Space Interferometry Mission (Shao 1998), the US Naval Observatory Full-Sky Astrometric Mapping Explorer (Horner et al. 2000) and the European Space Agency's Global Astrometric Interferometer for Astrophysics (Perryman et al. 2001) will achieve microarcsecond positional accuracies, requiring new definitions of the ICRS.

The authors thank the many NRAO, GSFC, and USNO staff members who offered advice and assistance during this work. The National Radio Astronomy Observatory is a facility of the National Science Foundation operated under cooperative agreement by Associated Universities, Inc. A. P. is grateful to the New Mexico Space Grant Consortium for partial support during this project.

REFERENCES

Altamimi, Z., Sillard, P., & Boucher, C. 2002, J. Geophys. Res., in press
Bartel, N., et al. 2000, Science, 287, 112
Beasley, A. J., & Conway, J. E. 1995, ASP Conf. Ser. 82, Very Long Baseline Interferometry and the VLBA, ed. J. A. Zensus, P. J. Diamond, & P. J. Napier (San Francisco: ASP), 328
Beasley, A. J., & Güdel, M. 2000, ApJ, 529, 961
Brisken, W. F., Benson, J. M., Beasley, A. J., Fomalont, E. B., Goss, W. M., & Thorsett, S. E. 2000, ApJ, 541, 959
Browne, I. W. A., Wilkinson, P. N., Patnaik, A. R., & Wrobel, J. M. 1998, MNRAS, 293, 257
Charlot, P. 1990, AJ, 99, 1309
Condon, J. J., & Broderick, J. J. 1985, AJ, 90, 2540
———. 1986, AJ, 91, 1051
Condon, J. J., Broderick, J. J., & Seielstad, G. A. 1989, AJ, 97, 1064
Condon, J. J., Cotton, W. D., Greisen, E. W., Yin, Q. F., Perley, R. A., Taylor, G. B., & Broderick, J. J. 1998, AJ, 115, 1693
Eubanks, T. M. 1993, in Contributions of Space Geodesy to Geodynamics: Earth Dynamics, ed. D. E. Smith & D. L. Turcotte (Washington: Amer. Geophys. Union), 1
Fassnacht, C. D., & Taylor, G. B. 2001, AJ, 122, 1661
Fey, A. L., & Charlot, P. 2000, ApJS, 128, 17
Fricke, W., et al. 1988, Veroff. Astron. Rechen-Instituts Heidelberg, 32, 1
Garrett, M. A., et al. 2001, A&A, 366, L5
Herrnstein, J. R., et al. 1999, Nature, 400, 539
Horner, S. D., et al. 2000, Proc. SPIE, 4013, 473
IERS. 1999, Ann. Rep., ed. D. Gambis (Paris: Obs. Paris), 87
King, L. J., Browne, I. W. A., Marlow, D. R., Patnaik, A. R., & Wilkinson, P. N. 1999, MNRAS, 307, 225
Kovalevsky, J., et al. 1997, A&A, 323, 620
Ma, C., & Feissel, M. 1997, IERS Tech. Note 23
Ma, C., et al. 1998, AJ, 116, 516
McCarthy, D. D. 1996, IERS Tech. Note, 21, 1
Napier, P. J. 1994, IAU Symp. 158, Very High Angular Resolution Imaging, ed. J. G. Robertson & W. J. Tango (Dordrecht: Kluwer), 117
Patnaik, A. R., Browne, I. W. A., Walsh, D., Chaffee, F. H., & Foltz, C. B. 1992a, MNRAS, 259, 1P
Patnaik, A. R., Browne, I. W. A., Wilkinson, P. N., & Wrobel, J. M. 1992b, MNRAS, 254, 655
Peck, A. B., & Taylor, G. B. 2000, ApJ, 534, 90
Peck, A. B., Taylor, G. B., Fassnacht, C. D., Readhead, A. C. S., & Vermeulen, R. C. 2000, ApJ, 534, 104
Perryman, M. A. C., et al. 1997, A&A, 323, L49
———. 2001, A&A, 369, 339
Press, W. H., Teukolsky, S. A., Vetterling, W. T., & Flannery, B. P. 1992, Numerical Recipes in C (2d ed.; Cambridge: Cambridge Univ. Press)
Reid, M. J., Readhead, A. C. S., Vermeulen, R. C., & Treuhaft, R. N. 1999, ApJ, 524, 816
Ryan, J. W., Clark, T. W., Ma, C., Gordon, D., Caprette, D. S., & Himwich, W. E. 1993, in Contributions of Space Geodesy to Geodynamics: Earth Dynamics, ed. D. E. Smith & D. L. Turcotte (Washington: Amer. Geophys. Union), 37
Shao, M. 1998, Proc. SPIE, 3350, 536
Sovers, O. J., Fanselow, J. L., & Jacobs, C. 1998, Rev. Mod. Phys., 70, 1393
Taylor, G. B., Beasley, A. J., Frail, D. A., Kulkarni, S. R., & Reynolds, J. E. 1999, A&AS, 138, 445
Wilkinson, P. N., Browne, I. W. A., Patnaik, A. R., Wrobel, J. M., & Sorathia, B. 1998, MNRAS, 300, 790
Wilkinson, P. N., et al. 2001, Phys. Rev. Lett., 86, 584